Extinction ratio and resonant wavelength tuning using three dimensions of silica microresonators

Song Zhu, Yang Liu, Lei Shi,* Xinbiao Xu, and Xinliang Zhang

Wuhan National Laboratory for Optoelectronics, Huazhong University of Science and Technology, Wuhan 430074, China
**Corresponding author: lshi@hust.edu.cn*

Received June 24, 2016; revised August 10, 2016; accepted August 13, 2016; posted August 17, 2016 (Doc. ID 269140); published September 16, 2016

In this paper, a multidimensional tuning method of the silica microcapillary resonator (MCR) is proposed and demonstrated whereby the extinction ratio (ER) as well as the resonant wavelength can be individually controlled. An ER tuning range of up to 17 dB and a maximum tuning sensitivity of 0.3 dB/μm are realized due to the tapered profile of the silica optical microfiber (MF) when the MF is adjusted along its axial direction. Compared to direct tuning of the coupling gap, this method could lower the requirement for the resolution of displacement stage to micrometers. When the MF is adjusted along the axial direction of the silica microcapillary, a resonance shift of 3.06 nm and maximum tuning sensitivity of 0.01 nm/μm are achieved. This method avoids the use of an applied external field to control the silica microresonators. Moreover, when air is replaced by ethanol and water in the core of the silica microcapillary, a maximum resonance shift of 5.22 nm is also achieved to further enlarge the resonance tuning range. Finally, a microbubble resonator with a higher Q factor is also fabricated to achieve an ER tuning range of 8.5 dB. Our method fully takes advantage of the unique structure of the MCR to separately and easily tune its key parameters, and may broaden its applications in optical signal processing and sensing.

OCIS codes: (230.5750) Resonators; (230.3990) Micro-optical devices; (170.4520) Optical confinement and manipulation.
http://dx.doi.org/10.1364/PRJ.4.000191

1. INTRODUCTION

In recent years, whispering-gallery mode (WGM) optical microresonators have attracted much attention and shown great potential [1–7]. Due to their high Q factor and sensitivity, silica whispering-gallery microresonators have been widely applied in various applications such as lasers [8–12], sensing [13–18], biomolecular and single nanoparticle detection [19–21], nonlinear optics [22,23], signal processing [23], and optomechanics [24–27]. Since the spectrum tunability plays a significant role in enhancing the flexibility of the silica whispering-gallery microresonators, the resonance tuning of the microresonators has been demonstrated. A resonance tuning of WGMs in the silica microsphere by changing the exerted electrostatic field strength was demonstrated by Ioppolo *et al.* [28], but the tuning range was only tens of picometers. As a result, other methods of tuning the resonant wavelength were investigated such as thermally assisted chemical etching and mechanical stretching [29–33]. In order to realize a larger tuning range, a microbubble resonator with wall thickness of 3 μm was fabricated to realize a mechanical tuning range of about 5.5 nm [34]. Also, by combination with the stretchable ability of polydimethylsiloxane (PDMS), the polymeric spherical microresonator was fabricated to tune the resonant wavelength with a range of 15 nm [35]. Using the same method, high-Q PDMS microresonators were fabricated to realize a broad strain tuning range of 50 nm [36]. Additionally, based on the photothermal effect, a novel silica microsphere resonator embedded with iron-oxide nanoparticles, which realized a large tuning range of over 13 nm and tuning sensitivity of 0.2 nm/mW, was demonstrated in our previous work [37]. Apart from microsphere resonators, the silica microcapillary resonator (MCR) has been used as one kind of WGM microresonator for tuning the resonant wavelength. In order to achieve practical application, an all-optical tuning scheme for silica MCRs was reported in another of our previous works [38], and a tuning range of 3.3 nm and tuning sensitivity of 0.15 nm/mW were achieved.

Since there is a weak Kerr effect and a lack of plasma dispersion effect in silica, it is difficult to realize the tunability of WGMs in the silica microresonators. The hollow core of the silica microcapillary has been used as one dimension for achieving the tuning of the MCRs. However, the previous work [38] only focused on this dimension to control the resonant wavelength, excluding the other parameters by using relatively complex procedures. In this work, a three-dimensional tuning method of the silica MCRs is proposed and demonstrated. Here, the silica microcapillaries and optical microfibers (MFs) we fabricated both possess tapered profiles.

A schematic view of the device and operation principle is illustrated in Fig. 1. The tapered profiles open up new tuning dimensions to control the silica MCRs. The extinction ratio (ER) tuning can be achieved when the microcapillary couples with the MF at different spots along the gradient profile of the MF, which can be utilized to realize the application in signal process such as order-tunable photonic differentiator and filters. Besides, there is also a tapered profile on the drawn silica microcapillary; thus, it can be used to realize resonant wavelength tuning when the coupling spot moves along the axial

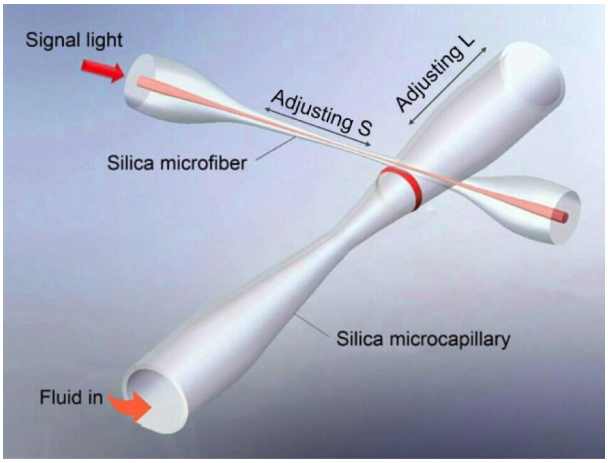

Fig. 1. Schematic diagram of the multidimensional tuning method. The waist of the MF is about 1 μm and the minimum outer diameter of the silica microcapillary is about 53 μm with a wall thickness of about 2.5 μm.

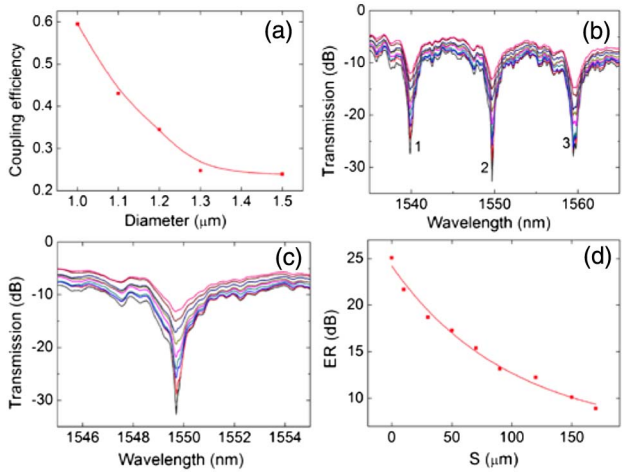

Fig. 2. (a) Coupling efficiency as a function of the fiber taper diameter. (b) Transmission spectra of the silica MCR at different coupling spots along the gradient profile of the MF (moving distance S is 0, 10, 30, 50, 70, 90, 120, 150, and 170 μm, respectively, from high to low ER). (c) Transmission spectra of the silica MCR at around 1550 nm. (d) ER tuning as a function of the moving distance S.

direction of the microcapillary. We also predict that the resonance tunability can be achieved by changing the liquid refractive index (RI) within the core of the silica microcapillary, which can further enlarge the wavelength tuning range, which can then be used in applications including the tunable filter. This tuning method sufficiently makes use of the unique structure of the MCR to separately and easily tune its main parameters and realize a relatively large tuning range and high tuning sensitivity.

2. DEVICE FABRICATION

A bare silica microcapillary has an outer diameter of 140 μm and inner diameter of 100 μm. In order to get a silica microcapillary with a tapered profile and thinner wall, it is necessary to treat it carefully. Since there were polyimide coatings on the outer surface of the silica microcapillary, the coatings were stripped by a hydrogen flame heating technology. After the bare silica microcapillary was heated by the flame, a syringe was used to pump air into the core of the microcapillary. Then a microcapillary with a minimum outer diameter of about 53 μm was drawn from the original microcapillary with an outer diameter of 140 μm. The wall thickness of the drawn silica microcapillary was about 2.5 μm. Since there were residues of the polyimide coatings on the outer surface of the silica microcapillary, ethanol was used to clean the residues.

Silica optical MFs were fabricated from standard single-mode fibers (SMFs), and an improved flame-heated technique was adopted to draw the SMFs into MFs [38,39]. The tapered profile of the MF could be used to tune the ER of the transmission spectrum of the silica MCR.

3. EXPERIMENTAL RESULTS AND DISCUSSION

The ER is determined by the coupling efficiency between the MF and the silica microcapillary. The coupling efficiency can be influenced not only by the gap between the MF and the silica microcapillary, but also the diameter of the MF. Direct accurate tuning of the coupling gap requires a high-resolution displacement stage. The resolution of our displacement stage is 1 μm, and thus it can't meet the requirement of direct accurate adjustment of the gap. In this work, a new ER tuning method is proposed. The MF is deposited perpendicularly to and keeps in touch with the silica microcapillary to excite the WGMs of the silica MCR. We can find that the coupled MF possesses a tapered profile which provides a gradient in radius. The gradient of the MF radius indicates a gradient in coupling coefficient between the MF and the silica microcapillary because variant taper radius is related to the evanescent light field. Therefore, the tapered profile indicates that the coupling efficiency can be tuned by just slightly adjusting the silica MF along its axial direction. This is analyzed by numerical calculation according to previous theory [40], as illustrated in Fig. 2(a). When the diameter of the MF increases, the evanescent light field outside the MF decreases, and so the coupling efficiency tends to decrease. Accordingly, it can be predicted that this method can accurately control the ER of the transmission spectrum almost without resonant wavelength shift.

The experimental result is shown in Figs. 2(b)–2(d). From Fig. 2(b), we note that there is only one evident dip in the free spectral range (FSR). Resonance dip 1, 2, and 3 denote the fundamental WGMs of the silica MCR, whereas the higher-order WGMs are almost negligible. Additionally, there exists one split for the resonance at around 1560 nm due to the interference between the fundamental mode and the higher-order mode [41,42]. In contrast to the fundamental WGMs, the evanescent field of the higher-order modes penetrates more into the core of the microcapillary so that the higher-order modes undergo larger bending loss and absorption loss than those of the fundamental WGMs. Moreover, the drawn silica microcapillary has a smaller diameter and thinner wall compared to a bare one. This leads to greater loss of the higher-order WGMs and consequently smoother transmission spectra. A fundamental WGM around 1550 nm was selected with the maximum ER of about 25 dB. In this work, the ER tuning range of up to 17 dB is achieved as the MF is moved along its axial direction. In Fig. 2(c), the minimum ER is about 8 dB. According to Fig. 2(a), we predict that the ER will tend to zero when the MF is adjusted to the coupling spot where the taper diameter of the MF is large enough.

According to our requirement, the MF moving direction should be perpendicular to the axial direction of the silica microcapillary. There is no displacement along the axial direction of the silica microcapillary when the MF is adjusted along its axial direction. It is a prerequisite that there be no wavelength shift while the ER varies. In Fig. 2(c), as the ER changes, the resonant wavelength experiences a very slight shift at around 1550 nm. At the same time, the bandwidth ($\delta\lambda$) decreases with the decreasing of the ER, and thus the Q factor increases moderately with the increase of moving distance (S), because it is in the process from overcoupling to undercoupling. Furthermore, according to Fig. 2(b), the MF moving distance S is 170 μm and corresponding continuous tuning range is 17 dB. The maximum tuning sensitivity of 0.3 dB/μm is achieved—that is to say, when the MF moves a distance of 1 μm, a tuning resolution of 0.3 dB can be achieved. High-resolution ER tuning is impossible to achieve by tuning the gap directly based on our 1 μm resolution displacement stage. Besides, according to Fig. 2(d), the slope varies at different moving distances because the slope of the taper is not uniform along the axial direction of the MF. Moreover, according to Fig. 2(a), with the increase of the MF taper diameter, the coupling efficiency decreases more and more slowly. We predict that the resolution of the ER tuning tends to be higher when the tapered profile of the MF becomes flatter.

Apart from the ER tuning, the resonance of the WGMs in the silica microresonator has been studied a lot in previous work. Here, a simple resonance-tuning method is demonstrated, as shown in Fig. 1. After the silica microcapillary is drawn from the outer diameter of 140 to 53 μm, the tapered silica microcapillary possesses a gradient profile in radius. The resonance of the WGMs in the silica microcapillary is approximately described as $2\pi R \cdot n_{\text{eff}} = m\lambda$, where R is the outer radius of the silica microcapillary at the coupling spot, n_{eff} is the effective RI, λ is the resonant wavelength in vacuum, and m is the angular number as an integer. When the MF moves along the axial direction of the silica microcapillary, the coupling spot between the MF and the silica microcapillary changes. Because of the tapered profile of the silica microcapillary, R varies with the coupling spot. Here, moving distance (L) of the MF along the axial direction of the silica microcapillary is considered as the foremost influencing factor on R. Thus, the relation between L, R, and the resonance shift $\Delta\lambda$ can be described by

$$\Delta\lambda = \frac{\lambda}{R} \cdot \frac{\partial R}{\partial L} \cdot \Delta L. \tag{1}$$

Equation (1) reflects that the resonance shift $\Delta\lambda$ can be controlled by the moving distance L. It can be seen that λ will increase with the moving distance L of the MF along the axial direction of the silica microcapillary; it is consistent with the results of experiments presented in Fig. 3.

According to Fig. 3, when the moving distance L is 560 μm, the corresponding resonance shift is 3.06 nm with a small change of the ER, realizing a relatively large tuning range and maximum tuning sensitivity of 0.01 nm/μm. Apart from that, when the MF moves along the tapered profile of the silica microcapillary, the wavelength tuning rate varies because there is a trend that the diameter of the microcapillary at different coupling spots increases more and more quickly. We predict

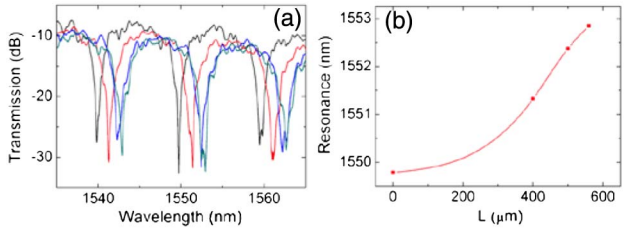

Fig. 3. (a) Transmission spectra of the silica MCR at different coupling spots along the gradient profile of the silica microcapillary (the moving distance L is 0, 400, 500, and 560 μm, respectively). (b) Resonance tuning as a function of the moving distance L.

that the resonant wavelength can shift at a higher resolution, as the silica microcapillary exhibits flatter tapered profile along the axial direction. In addition, the FSR gets slightly smaller in the process of the resonance tuning with increasing microcapillary diameter.

The resonance tuning range in the scheme just discussed is not large enough compared to the FSR. As shown in Fig. 1, the silica MCR has a natural fluidic channel. According to $2\pi R \cdot n_{\text{eff}} = m\lambda$, as the evanescent light field of the WGMs can experience the change in the RI induced by different liquid, the resonant wavelength can be tuned by replacing the liquid which flows through the core of the silica microcapillary. Therefore, the fluidic channel can be used as another dimension to enlarge the resonance tuning range. In order to analyze the extent of the interaction between fluid and WGMs, the distribution of the WGMs in the MCR ought to be presented. The electromagnetic waves inside a microcapillary can be described by solving the Helmholtz equation in cylindrical coordinates. The radial distribution of the WGM of an MCR can be described as [1]

$$E_{m,l}(r) = \begin{cases} AJ_m(k_0^{(l)} n_1 r) & (r \le r_1) \\ BJ_m(k_0^{(l)} n_2 r) + CH_m^{(1)}(k_0^{(l)} n_2 r) & (r_1 < r \le r_2) \\ DH_m^{(1)}(k_0^{(l)} n_3 r) & (r > r_2) \end{cases}, \tag{2}$$

where J_m and $H_m^{(1)}$ are the Bessel and Hankel functions of the first kind, respectively, with mth. The RIs of the core, wall, and medium outside are described by n_1, n_2, and n_3. r_1 and r_2 represent the inner and outer radius of the microcapillary, respectively. $k_0^{(l)}$ represents the amplitude of the resonance wave vector in vacuum with order l. A, B, C, and D are determined by the boundary conditions. The extent to which the WGM interacts with the fluid within the core depends on the wall thickness and the order of the WGMs. The fundamental WGM is considered in this work and the method for decreasing the wall thickness is adopted to improve the fluidic tuning performance. The modes of WGM structures can be determined using COMSOL. Figures 4(a)–4(d) show the mode distributions of the MCR with wall thickness of 20 and 2.5 μm, respectively. We observe that the WGM in the MCR with smaller wall thickness has larger overlap with fluid within the core, and the percentage of the WGM in the core was found by integrating the field in the core and wall of the microcapillary, as shown in Fig. 4(e). We find that the energy percentage of the WGMs in the core increases with the decreasing of the wall thickness. As a result, the extent of the

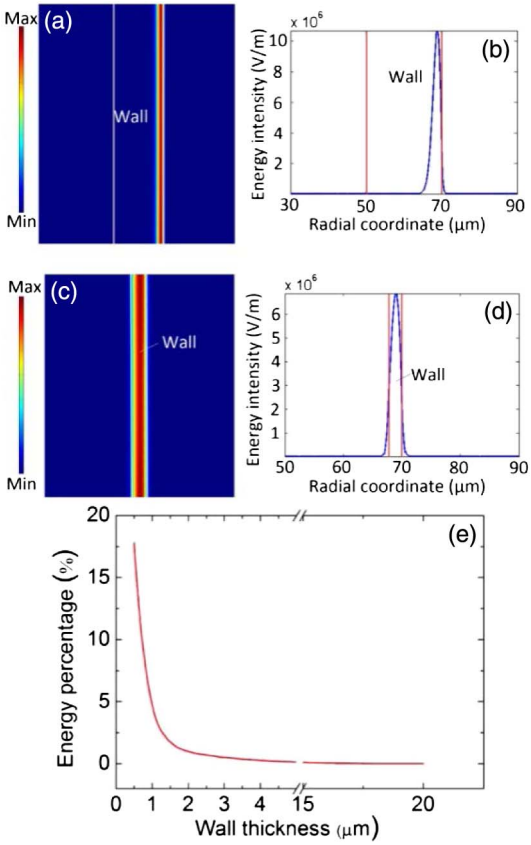

Fig. 4. Electric field in the MCR with wall thickness of (a), (b) 20 μm and (c), (d) about 2.5 μm. (e) Energy percentage of the WGM in the core as a function of the microcapillary wall thickness for the fundamental mode.

interaction between the mode and the fluid in the core is larger, leading to greater tuning range and higher sensitivity.

Experiments were carried out to test the feasibility of the resonance tuning by changing the RI within the silica microcapillary. The original silica microcapillary has a wall thickness of 20 μm. According to Fig. 4(e), when the WGMs circulate in the wall, the vast majority of the light is confined within the wall and the evanescent field penetrating into the core is very small; thus, it is indispensable to decrease the wall thickness. According to the method we just mentioned, the wall thickness could be decreased to about 2.5 μm. Here, ethanol was utilized to replace air with the help of a syringe. The RI of ethanol is 1.36 at 1550 nm. The relation between n_{eff}, n_{core}, and the resonance shift $\Delta\lambda$ can be described as

$$\Delta\lambda = \frac{\lambda}{n_{\text{eff}}} \cdot \frac{\partial n_{\text{eff}}}{\partial n_{\text{core}}} \cdot \Delta n_{\text{core}}, \tag{3}$$

where n_{core} represents the RI in the core of the silica microcapillary. With the increase of n_{core}, n_{eff} of the WGM increases and a redshift happens. The resonance shift of the WGM is shown in Fig. 5(a). We observe that a resonance shift of 1.42 nm was achieved. At last, in order to further verify the influence of the decreasing wall thickness and enlarge the fluidic tuning range, another MCR was fabricated with wall thickness of about 2 μm. Figure 5(b) shows the resonance shift when water and ethanol, respectively, were pumped into

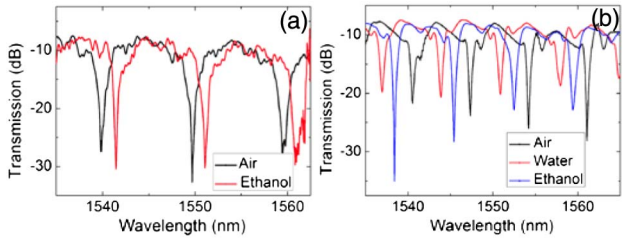

Fig. 5. Resonance tuning of the silica MCR with wall thickness of (a) about 2.5 μm and (b) about 2 μm.

the core, with a maximum tuning range up to 5.22 nm. We predict that the fluidic channel possesses the potential to tune the resonant wavelength for a large range. Hence, a larger resonance tuning range can be realized using this simple method.

4. PERFORMANCE LIMITATION

The low Q factor mainly results from weak confinement of WGMs along the axial direction of the MCR, the overcoupling state between the MF and the MCR, and the residues on the surface of the microcapillary. Since the coupling regime between the MF and the MCR is located in the taper area of the drawn capillary, the WGMs' light cannot be confined along the axial direction of the capillary, which will increase the loss of the WGMs in the resonator and leads to degradation of the Q factor [13]. Moreover, in order to stably adjust the coupling MF, the MF is in touch with the MCR, which will lead to overcoupling and reduction of the Q factor [43–45]. Since the polyimide coatings on the outer surface of the microcapillary are stripped by a hydrogen flame heating technology, the residues could induce the scattering loss.

In order to improve the Q factor, the microbubble resonator is fabricated due to the RI limitation along the axial direction of it [17], as shown in Fig. 6(a). The transmission spectrum of the microbubble resonator is measured through the optical spectrum analyzer with a resolution of 0.02 nm, as shown in Fig. 6(b). A Q factor of over 5.2×10^4 is realized, which is close to the resolution of the optical spectrum analyzer.

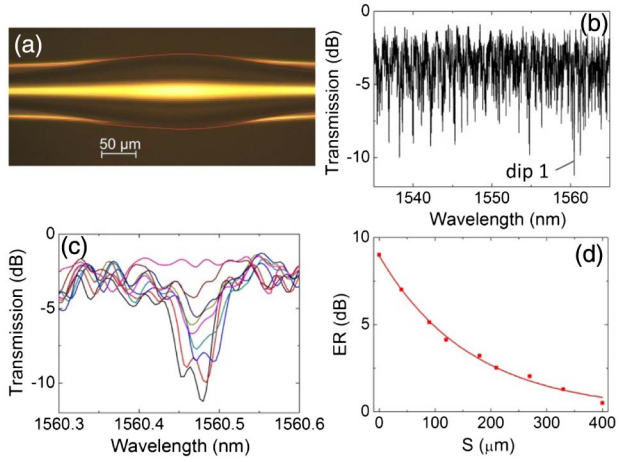

Fig. 6. (a) Optical microscopic image of the microbubble resonator. (b) Transmission spectrum of the microbubble resonator. (c) ER tuning of a resonance around 1560.5 nm (the moving distance S is 0, 40, 90, 120, 180, 210, 270, 330, and 400 μm, respectively, from high to low ER). (d) ER tuning as a function of the moving distance S.

The very large mode density results from the strong asphericity of the bottle-like resonator [46], and thus it is difficult to measure the resonance-tuning range by adjusting the MF with our present displacement stage. ER tuning with the higher Q factor of 5.2×10^4 (dip 1) is carried out, as shown in Figs. 6(c) and 6(d), and a tuning range of 8.5 dB is achieved. Therefore, high-Q WGMs tuning can be experimentally realized and the low-Q resonance is utilized to verify the possibility of large wavelength and ER tuning range.

5. CONCLUSION

In summary, we propose a novel method to control the ER and resonance individually based on three dimensions of silica MCRs. By adjusting the MF along its axial direction, an ER tuning range of 17 dB and maximum tuning sensitivity of 0.3 dB/μm were achieved. At another dimension, a resonant wavelength shift of 3.06 nm with a maximum tuning sensitivity of 0.01 nm/μm was realized, owing to the coupling spot varying along the axial direction of the silica microcapillary. Apart from that, another resonance shift of 5.22 nm was obtained by injecting ethanol into the core in order to further enlarge the wavelength tuning range. In order to improve the Q factor, the microbubble resonator was fabricated to realize an ER tuning range of 8.5 dB with a Q factor of 5.2×10^4. Thus, the multidimensional method can be regarded as a versatile approach to separately tuning the main parameters of the silica MCRs, which can be utilized in applications such as tunable filters and order-tunable photonic differentiators.

Funding. National Natural Science Foundation of China (NSFC) (61307075); Specialized Research Fund for the Doctoral Program of Higher Education of China (20120142120067); Fundamental Research Funds for the Central Universities (HUST: 2014TS019); Director Fund of Wuhan National Laboratory for Optoelectronics.

REFERENCES

1. I. M. White, H. Oveys, and X. Fan, "Liquid-core optical ring-resonator sensors," Opt. Lett. **31**, 1319–1321 (2006).
2. Q. Lu, M. Li, J. Liao, S. Liu, X. Wu, L. Liu, and L. Xu, "Strong coupling of hybrid and plasmonic resonances in liquid core plasmonic micro-bubble cavities," Opt. Lett. **40**, 5842–5845 (2016).
3. L. Zou, Y. Huang, X. Lv, B. Liu, H. Long, Y. Yang, J.-L. Xiao, and Y. Du, "Modulation characteristics and microwave generation for AlGaInAs/InP microring lasers under four-wave mixing," Photon. Res. **2**, 177–179 (2014).
4. M. S. Murib, E. Yüce, O. Gürlü, and A. Serpengüze, "Polarization behavior of elastic scattering from a silicon microsphere coupled to an optical fiber," Photon. Res. **2**, 45–50 (2014).
5. W. Jin, X. Yi, Y. Hu, B. Li, and Y. Xiao, "Temperature-insensitive detection of low-concentration nanoparticles using a functionalized high-Q microcavity," Appl. Opt. **52**, 155–161 (2013).
6. B. Li, Y. Xiao, C. Zou, X. Jiang, Y. Liu, F. Sun, Y. Li, and Q. Gong, "Experimental controlling of Fano resonance in indirectly coupled whispering-gallery microresonators," Appl. Phys. Lett. **100**, 021108 (2012).
7. N. Singh, D. D. Hudson, R. Wang, E. C. Mägi, D.-Y. Choi, C. Grillet, B. L. Davies, S. Madden, and B. J. Eggleton, "Positive and negative phototunability of chalcogenide (AMTIR-1) microdisk resonator," Opt. Express **23**, 8681–8686 (2015).
8. X. Jiang, C. Zou, L. Wang, Q. Gong, and Y. Xiao, "Whispering-gallery microcavities with unidirectional laser emission," Laser Photon. Rev. **10**, 40–61 (2016).
9. T. Kippenberg, S. Spillane, D. Armani, and K. Vahala, "Ultralow-threshold microcavity Raman laser on a microelectronic chip," Opt. Lett. **29**, 1224–1226 (2004).
10. A. François, N. Riesen, K. Gardner, T. M. Monro, and A. Meldrum, "Lasing of whispering gallery modes in optofluidic microcapillaries," Opt. Express **24**, 12466–12477 (2016).
11. X. Jiang, Y. Xiao, Q. Yang, L. Shao, W. R. Clements, and Q. Gong, "Free-space coupled, ultralow-threshold Raman lasing from a silica microcavity," Appl. Phys. Lett. **103**, 101102 (2013).
12. B. Li, W. R. Clements, X. Yu, K. Shi, Q. Gong, and Y. Xiao, "Single nanoparticle detection using split-mode microcavity Raman lasers," Proc. Natl. Acad. Sci. USA **111**, 14657–14662 (2014).
13. V. Zamora, A. Díez, M. V. Andrés, and B. Gimeno, "Refractometric sensor based on whispering-gallery modes of thin capillaries," Opt. Express **15**, 12011–12016 (2007).
14. S. Lane, P. West, A. François, and A. Meldrum, "Protein biosensing with fluorescent microcapillaries," Opt. Express **23**, 2577–2590 (2015).
15. A. Lee, T. Mills, and Y. Xu, "Nanoscale welding aerosol sensing based on whispering gallery modes in a cylindrical silica resonator," Opt. Express **23**, 7351–7365 (2015).
16. J. Knittel, J. D. Swaim, D. L. McAuslan, G. A. Brawley, and W. P. Bowen, "Back-scatter based whispering gallery mode sensing," Sci. Rep. **3**, 2974 (2013).
17. Y. Yang, S. Saurabh, J. M. Ward, and S. N. Chormaic, "High-Q, ultrathin-walled microbubble resonator for aerostatic pressure sensing," Opt. Express **24**, 294–299 (2015).
18. T. Reynolds, M. R. Henderson, A. François, N. Riesen, J. M. M. Hall, S. V. Afshar, S. J. Nicholls, and T. M. Monro, "Optimization of whispering gallery resonator design for biosensing applications," Opt. Express **23**, 17067–17076 (2015).
19. S. Arnold, M. Khoshsima, I. Teraoka, S. Holler, and F. Vollmer, "Shift of whispering-gallery modes in microspheres by protein adsorption," Opt. Lett. **28**, 272–274 (2003).
20. J. Zhu, S. K. Ozdemir, Y. Xiao, L. Li, L. He, D. Chen, and L. Yang, "On-chip single nanoparticle detection and sizing by mode splitting in an ultrahigh-Q microresonator," Nat. Photonics **4**, 46–49 (2010).
21. L. Shao, X. Jiang, X. Yu, B. Li, W. R. Clements, F. Vollmer, W. Wang, Y. Xiao, and Q. Gong, "Detection of single nanoparticles and lentiviruses using microcavity resonance broadening," Adv. Mater. **25**, 5616–5620 (2013).
22. N. Riesen, W. Zhang, and T. M. Monro, "Dispersion analysis of whispering gallery mode microbubble resonators," Opt. Express **24**, 8832–8847 (2016).
23. M. Pöllinger and A. Rauschenbeutel, "All-optical signal processing at ultra-low powers in bottle microresonators using the Kerr effect," Opt. Express **18**, 17764–17775 (2010).
24. C. Dong, Z. Shen, C. Zou, Y. Zhang, W. Fu, and G. Guo, "Brillouin-scattering-induced transparency and non-reciprocal light storage," Nat. Commun. **6**, 6193 (2014).
25. K. Han, J. H. Kim, and G. Bahl, "Aerostatically tunable optomechanical oscillators," Opt. Express **22**, 1267–1276 (2014).
26. X. Jiang, M. Wang, M. C. Kuzyk, T. Oo, G. Long, and H. Wang, "Chip-based silica microspheres for cavity optomechanics," Opt. Express **23**, 27260–27265 (2015).
27. Z. Shen, Z. Zhou, C. Zou, F. Sun, G. Guo, C. Dong, and G. Guo, "Observation of high-Q optomechanical modes in the mounted silica microspheres," Photon. Res. **3**, 243–247 (2015).
28. T. Ioppolo, U. Ayaz, and M. V. Ötügen, "Tuning of whispering gallery modes of spherical resonators using an external electric field," Opt. Express **17**, 16465–16479 (2009).
29. A. Watkins, J. Ward, and S. N. Chormaic, "Thermo-optical tuning of whispering gallery modes in Erbium: Ytterbium doped glass microspheres to arbitrary probe wavelengths," Jpn. J. Appl. Phys. **51**, 052501 (2012).
30. I. M. White, N. M. Hanumegowda, H. Oveys, and X. Fan, "Tuning whispering gallery modes in optical microspheres with chemical etching," Opt. Express **13**, 10754–10759 (2005).
31. W. V. Klitzing, R. Long, V. S. Ilchenko, J. Hare, and V. Lefevre-Seguin, "Frequency tuning of the whispering-gallery modes of silica microspheres for cavity quantum electrodynamics and spectroscopy," Opt. Lett. **26**, 166–168 (2001).
32. V. S. Ilchenko, P. S. Volikov, V. L. Velichansky, F. Treussart, V. L. Seguin, J.-M. Raimond, and S. Haroche, "Strain-tunable high-Q optical microsphere resonator," Opt. Commun. **145**, 86–90 (1998).

33. K. N. Dinyari, R. J. Barbour, D. A. Golter, and H. Wang, "Mechanical tuning of whispering gallery modes over a 0.5 THz tuning range with MHz resolution in a silica microsphere at cryogenic temperatures," Opt. Express **19**, 17966–17972 (2011).
34. M. Sumetsky, Y. Dulashko, and R. S. Windeler, "Super free spectral range tunable optical microbubble resonator," Opt. Lett. **35**, 1866–1868 (2010).
35. R. Madugani, Y. Yang, J. M. Ward, J. D. Riordan, S. Coppola, V. Vespini, S. Grilli, A. Finizio, P. Ferraro, and S. N. Chormaic, "Terahertz tuning of whispering gallery modes in a PDMS stand-alone, stretchable microsphere," Opt. Lett. **37**, 4762–4764 (2012).
36. Z. Zhou, F. Shu, Z. Shen, C. Dong, and G. Guo, "High-*Q* whispering gallery modes in a polymer microresonator with broad strain tuning," Sci. Chin. Phys. Mech. Astron. **58**, 114208 (2015).
37. P. Zhao, L. Shi, Y. Liu, Z. Wang, S. Pu, and X. Zhang, "Iron-oxide nanoparticles embedded silica microsphere resonator exhibiting broadband all-optical wavelength tunability," Opt. Lett. **39**, 3845–3848 (2014).
38. Y. Liu, L. Shi, X. Xu, P. Zhao, Z. Wang, S. Pu, and X. Zhang, "All-optical tuning of a magnetic-fluid-filled optofluidic ring resonator," Lab Chip **14**, 3004–3010 (2014).
39. X. Yu, B. Li, P. Wang, L. Tong, X. Jiang, Y. Li, Q. Gong, and Y. Xiao, "Single nanoparticle detection and sizing using a nanofiber pair in an aqueous environment," Adv. Mater. **25**, 5616–5620 (2013).
40. Y. Liu, T. Chang, and A. E. Craig, "Coupled mode theory for modeling microring resonators," Opt. Eng. **44**, 084601 (2005).
41. S. J. Emelett and R. A. Soref, "Analysis of dual-microring-resonator cross-connect switches and modulators," Opt. Express **13**, 7840–7853 (2005).
42. L. Y. Mario and M. K. Chin, "Optical buffer with higher delay-bandwidth product in a two-ring system," Opt. Express **16**, 1796–1807 (2008).
43. M. L. Gorodetsky and V. S. Ilchenko, "Optical microsphere resonators: optimal coupling to high-*Q* whispering-gallery modes," J. Opt. Soc. Am. B **16**, 147–154 (1999).
44. M. Cai, O. Painter, and K. J. Vahala, "Observation of critical coupling in a fiber taper to a silica-microsphere whispering-gallery mode system," Phys. Rev. Lett. **85**, 74–77 (2000).
45. C. Zou, Y. Yang, C. Dong, Y. Xiao, X. Wu, Z. Han, and G. Guo, "Taper-microsphere coupling with numerical calculation of coupled-mode theory," J. Opt. Soc. Am. B **25**, 1895–1898 (2008).
46. G. S. Murugan, J. S. Wilkinson, and M. N. Zervas, "Selective excitation of whispering gallery modes in a novel bottle microresonator," Opt. Express **17**, 11916–11925 (2009).